

# The Effect of Confinement and Shear Connector on the Ultimate Capacity of the Short Composite Column

<sup>1</sup>Hadad Said Hadad, <sup>2</sup>Mohammed Taha Nooman and <sup>3</sup>Mostafa Mohammed Ahmed Mostafa

<sup>1</sup> Professor, Housing and Building National Research Center, Cairo, Egypt

<sup>2</sup> Dr., Al Azhar University, Faculty of Engineering, Cairo, Egypt

<sup>3</sup> Demonstrator, Al Azhar University, Faculty of Engineering, Qena, Egypt

**Abstract** - In recent years, the use of encased steel concrete composite columns has been increased significantly in medium or high-rise buildings. Most design codes and researches neglect effect of confinement and shear connectors. The study represents a qualitative transition in the experimental and analytical investigations on shear connectors effectively at steel concrete interfaces. The most studies in the field of shear connectors were devoted to composite beam and slab systems. The aim of the present investigation is to assess experimentally the current methods and codes for evaluating the ultimate load behavior of concrete encased steel short columns with the use of different stirrups ratio and shear connectors with different shapes and sizes to provide resistance to slip at steel concrete interfaces. In the present study nine specimens having a column cross section of (120x160) mm and a length of (800) mm were tested under axial loading. One specimen was chosen to be control column; some specimens were chosen to be strengthened by horizontal stirrups with different spacing ( $\emptyset 6$ ). The others specimens were chosen to be strengthened by horizontal shear connectors with different spacing and types. The test results show that the decreasing in spacing of stirrups technique gives an increase in the load carrying capacity up to (15 %) of the control ultimate capacity. However, using shear connectors system technique which made of steel reinforcement bars and stud shear connectors welded to flange of steel shape encased concrete gives an increase in the load carrying capacity up to (8.3%) of the control ultimate capacity. In addition, increasing numbers of horizontal stirrups increases the load carrying capacity of the encased composite columns under axial load. The results suggest that the effect of confinement and shear connectors should take in account for increasing the load carrying capacity, ductility and stiffness for column subjected to axial loading.

**Keywords** - Composite columns; Concrete encased columns; Confinement; Shear connectors.

## I. INTRODUCTION

For the past two decades, concrete encased steel columns are used in tall buildings. They have the rigidity and stiffness of concrete, as well as, the strength and ductility of the steel section. They also reduce the cross sectional dimensions which in turn makes them more slender and easy to erect. Composite columns can be classified as either hollow sections filled with concrete or steel sections encased in concrete. The latter one is considered in this paper. It offers high strength, ductility, fire protection for the steel section, and simplified beam to column connections. Different methods for the design of composite columns exist in codes of practice [1–8] with neglecting the effect of confinement and shear connectors in most codes of practice. A composite column may be treated in some methods as a steel column strengthened by concrete. On the other hand, it may be treated as a reinforced concrete column with special reinforcement. Furthermore, the strength of a composite column may be evaluated as the sum of strengths of both components, concrete and steel reinforcements. Existing code differences may be attributed to difference in design philosophy; i.e., strain distribution and compatibility. This discrepancy is referring to the differences in allowable material properties, limiting dimensions and safety factors [9–11].

The confinement of column by increasing horizontal stirrups number is one type of strengthening techniques to improve the behavior of the load carrying capacity of columns. Shear connectors can be performed by means of welding of reinforcement bars or studs in steel encased section to resist shear transfer at surface between steel and concrete. The present study deals with studying effects of confinement and shear connectors in the rectangular composite encased concrete columns (CEC) under axial loads using different stirrups numbers and shear connectors with different shapes and sizes.

K.Z. Soliman and others [12] investigated and evaluated the ultimate axial compression strength of the concrete encased steel columns and also the concrete contribution to the ultimate axial load according to the available different codes. Therefore, the encased steel sections were replaced with plastic pipes and wood shape S.I.B, instead of steel pipes and steel S.I.B sections. For each specimen, the loads carried by the concrete portion, steel portion, and the composite section were determined according to the available different codes [1–5] requirements. The used codes do not consider the confinement effect for predicting the ultimate axial strength of the columns. The comparative of studies with the experimental results showed that the predicted results are generally lower than the test results which means that the calculated column strengths using the five previous codes are almost on the conservative side. However, the ECP-SC-LRFD-2012 formula led to the most conservative results. The ultimate load and corresponding axial deformation of the tested columns varied depending on both the configuration of the lateral steel reinforcement and the encased steel shape which are not considered in the available design codes. *Mimoune* [13] studied

theoretically the monotonic behavior of composite columns under axial load and he concluded that the obtained results showed a difference between different codes of practice. It was also stated that, the confinement coefficients' values need to be adjusted.

*Paul and Samanta [14]* assessed the axial capacity of a concrete encased steel short column by two different codes, the Euro Code EC4 and the Load and Resistance Factor Design American Institute of Steel Construction AISC-LFRD code using a 3D finite element model. They reported that the Euro Code EC4 method shows more accurate predictions of composite column strength. However, neither EC4 nor AISC provisions explicitly consider any increase in the strength or ductility of concrete due to transverse ties, i.e.; the confinement effect was not included so it is of importance to experimentally investigate the concrete confinement effect on the concrete encased steel composite columns.

*A. K. Samanta and A. Paul [15]* presented the design assessment of concrete encased I-sections composite column based approaches given in Eurocode, ACI Code, BS. Code and AISC-LRFD. This study includes comparison of various design parameters and evaluation of design strength based on the procedures predicted in the various codes of practices .A practical example has been assumed and calculation has been shown to evaluate their potentiality in understanding in predicting the potentiality of various procedures. The obtained results based on the methods varies widely, because of the different design considerations adopted by the different codes. As such, they have hardly considered the effect of confinement of the concrete due to the presence of longitudinal reinforcements as well as lateral ties .

*L. K. Al- Hadithy and others [16]* used three types of shear connectors with four concrete grades for each type in fabricating composite specimens. The twelve composite prototypes were subjected to push out test individually to examine their behavior by measuring the slip values for each load incremental till failure, thus determining the resistance extent of each connectors type and specifying the failure mode at interface. A nonlinear three dimensional finite element analysis was carried out on twelve composite column segments using ANSYS computer program. Comparison of the experimental and theoretical results has shown good agreement that verifies the accuracy of the finite element model based on the smeared crack model of concrete. Results detected the development of the relative slip be at all ranges of the load-slip relationship at interface even with using effective shear connection and /or high quality concrete. The headed studs revealed the highest slip resistance and ultimate load over the channel and the L-shaped studs. The high strength concrete has also revealed the same superiority over the other three tested types of concrete.

### 1.1 Brief description of the available design codes for composite columns

Different concepts for the design of composite columns exist in the available codes of practice [1–8], will be summarized hereinafter:

#### 1.1.1. ECP 203-2007 [1]

The design of composite columns is based on the limit state design method with loading factors and partial safety for materials. The strength of a composite column is computed as for reinforced concrete members. Failure is defined in terms of a 0.002 strain limit for any concrete layer. However, the slenderness and area parameters are modified for the presence of the steel section. Load transfer should be provided by direct bearing at the connections. The load carried by the concrete shall not exceed the allowable bearing stress to avoid overstressing of concrete. The main equations used in the analysis are mentioned below for this code:

$$P_u = 0.35 f_{cu} A_c + 0.67 f_{ysc} A_{sc} \quad (\text{Concrete portion}) \quad (1)$$

$$P_u = 0.35 f_{cu} A_c + 0.67 f_{yss} A_{ss} + 0.67 f_{ysc} A_{sc} \quad (\text{Composite section}) \quad (2)$$

#### 1.1.2. ECP-Sc-LRFD-2012 [2]

It is based on limit state design with loading factors , partial safety for materials, modified yield stress, modified young's modulus, modified radius of gyration and numerical quantification. The design of composite columns is based on the design equations for steel columns. However, the slenderness and area parameters are modified for the presence of concrete. Load transfer should be provided by direct bearing at the connections. The load carried by the concrete shall not exceed the allowable bearing stress to avoid overstressing of concrete. The main equations used in the analysis are mentioned below for this code:

$$P_u = 0.80 A_s F_{cr} \quad (\text{Composite section}) \quad (3)$$

$$F_{cr} = \frac{0.648 F_{ym}}{\lambda^2} \quad \text{for } \lambda \geq 1.1 \quad (4)$$

$$F_{cr} = (1 - 0.348 \lambda_2) F_{ym} \quad \text{for } \lambda \leq 1.1; \text{ where } \lambda = \text{slenderness ratio} \quad (5)$$

$$F_{ym} = F_y + 0.7 F_{yr} * \frac{A_r}{A_s} + 0.48 * f_{cu} * \frac{A_c}{A_s} \quad (6)$$

#### 1.1.3. ACI-318-08 [3]

It uses the limit state design format with factors and capacity reduction factors. The strength of a composite column is computed as for reinforced concrete members. Failure is defined in terms of a 0.002 strain limit for any concrete layer. The expression for equivalent stiffness includes a creep factor, and cracked concrete stiffness is considered. Minimum eccentricities are specified to cover construction tolerances .The main equations used in the analysis are mentioned below for this code:

$$P_{n,max} = 0.80 [0.85 f_c' (A_g - A_{st}) + f_y A_{st}] \quad (\text{Concrete portion}) \quad (7)$$

$$P_{n,max} = 0.85 [0.85 f_c' (A_g - A_{st}) + f_{yss} A_{ss} + f_y A_{st}] \quad (\text{Composite section}) \quad (8)$$

#### 1.1.4. AISC-LRFD-2010 [4]

The load and resistance factor design uses the limit state design method with loading factors and capacity reduction factors. The design of composite columns is based on the design equations for steel columns. The slenderness and area parameters are

modified for the presence of concrete. Load transfer should be provided by direct bearing at the connections. The main equations used in the analysis are mentioned below for this code:

$$P_{no} = [0.85F_c A_c + F_y A_s + F_{ysr} A_{sr}] \quad (\text{Composite section}) \quad (9)$$

$P_{no}$  = nominal axial compressive strength without consideration of length effects,

$$P_e = \pi^2 (EI_{eff}) / (KL)^2 \quad (10)$$

$$P_n = 0.75 \times P_{no} \times [0.658 \frac{P_{no}}{P_e}] \quad , \quad \text{if } \frac{P_{no}}{P_e} \leq 2.25 \quad (11)$$

$$P_n = 0.877 P_e \quad , \quad \text{if } \frac{P_{no}}{P_e} > 2.25 \quad (12)$$

$$EI_{eff} = E_s I_s + 0.5 E_s I_{sr} + C_1 E_c I_c \quad (13)$$

$$C_1 = 0.1 + 2 \left( \frac{A_s}{A_s + A_c} \right) \leq 0.3 \quad (14)$$

#### LOAD TRANSFER

When the entire external force is applied directly to the concrete encasement or concrete fill, the force required to be transferred to the steel,  $V_r'$ , shall be determined as follows:

$$V_r' = P_r (F_y A_s / P_{no}) \quad (15)$$

where:  $P_r$  = required external force applied to the composite member, kips (N),  $V_r'$  = required shear force kips (N). It is necessary to ensure that load is transferred from the concrete to the steel by Shear Connectors, Shear strength of a connector:

$$Q_n = 0.5 A_{sa} \sqrt{f_c E_c} \leq A_{sc} F_u \quad (16)$$

Where:  $A_{sa}$  = cross-sectional area of steel headed stud, in.<sup>2</sup> (mm<sup>2</sup>),  $E_c$  = modulus of elasticity of concrete ksi (MPa),  $F_u$  = specified minimum tensile strength of a steel headed stud anchor, ksi (MPa)

#### 1.1.5. BS 5400-Part 5 [5]

It is based on limit state design with loading factors and partial safety for materials. Reduced concrete properties are used to account for the effect of creep and the use of the un-cracked concrete section in stiffness calculation. The slenderness parameter is consistent with the design of steel columns as the method reduces to the bare steel column design when the concrete portion is removed. The main equations used in the analysis are mentioned below for this code:

$$\alpha_c = \frac{0.45 \times A_c \times F_{cu}}{N_u} \quad (\text{concrete contribution ratio}) \quad (17)$$

$$N_u = 0.91 A_s f_y + 0.87 A_r f_{ry} + 0.45 A_c f_{cu} \quad (\text{Short column}) \quad (18)$$

$$N_{ay} = 0.85 K_{1y} N_u \quad \text{if } \alpha_c \text{ is not applicable (Composite column)} \quad (19)$$

#### 1.1.6. Chinese code CECS159[6]

CECS159 to predict the ultimate section capacity of a CFST stub column The predicted ultimate member capacity is:

$$N_{pl} = \chi N_{ps} \leq N_{ps}, \quad N_{ps} = A_s f_y / \gamma_s + A_{sr} f_{yr} / \gamma_{sr} + A_c f_c' / \gamma_c \quad (20)$$

Where  $\gamma_s = 1.1$  is the partial safety factor for structural steel,  $\gamma_{sr} = 1.15$  partial safety factor for steel reinforcement, the partial safety factor for concrete  $\gamma_c$  is 1.4 and the cylinder compressive strength  $f_c'$  is replaced by prism compressive strength  $f_{ck}$ .

$$\chi = 1 - 0.65 \lambda^2 \quad \text{for } \lambda \leq 0.215 \quad (21)$$

$$\chi = \frac{1}{2 \lambda^2} [(0.965 + 0.3 \lambda + \lambda^2) - \sqrt{(0.965 + 0.3 \lambda + \lambda^2)^2 - 4 \lambda^2}] \quad \text{for } \lambda > 0.215 \quad (22)$$

where the non-dimensional slenderness  $\lambda$  is defined as:

$$\lambda = \frac{l_e}{\pi} \sqrt{\frac{f_y A_s + f_{ck} A_c + f_{yr} A_{sr}}{E_s I_s + E_c I_c + E_{sr} I_{sr}}} \quad (23)$$

#### 1.1.7. Hong Kong code [7]

predicted ultimate section capacity is:

For fully encased and partially encased H sections:

$$N_{ps} = A_s f_y / \gamma_{m1} + A_{sr} f_{yr} / \gamma_{sr} + 0.45 A_c f_{cu} \quad (24)$$

For in filled rectangular hollow sections:

$$N_{ps} = A_s f_y / \gamma_{m1} + A_{sr} f_{yr} / \gamma_{sr} + 0.53 A_c f_{cu} \quad (25)$$

Where  $f_{cu}$  is the cube compressive strength of concrete,  $\gamma_{m1} = 1.1$  is the partial safety factor for structural steel,  $\gamma_{sr} = 1.15$  partial safety factor for steel reinforcement. The HKS approach is quite similar to the EC4 approach in predicting the member capacity of a composite column, except that it replaces 1.0 by 0.8 and  $f_c'$  by  $f_{cu}$  in calculating the nominal section capacity defined by this Eq.

$$N_u = f_y / \gamma_{m1} A_s + f_{yr} A_{sr} + v A_c f_c' \quad (26)$$

Where  $v = 1$  for a CFST and  $v = 0.85$  for encased column.

#### 1.1.8. Eurocode4 [8]

The predicted ultimate section capacity of composite columns stub column is:

$$N_{ps} = A_s f_y / \gamma_s + A_{sr} f_{yr} / \gamma_{sr} + v A_c f_c' / \gamma_c \quad (27)$$

Where  $\gamma_s = 1.0$  is the partial safety factor for structural steel,  $\gamma_{sr} = 1.15$  partial safety factor for steel reinforcement,  $\gamma_c = 1.5$  the partial safety factor for concrete, respectively,  $v = 1$  for a CFST and  $v = 0.85$  for encased column. The predicted ultimate member capacity of a slender composite column is:

$$N_{pl} = \chi N_{ps} \leq N_{ps} \quad (28)$$

$$\chi = \frac{1}{\phi + \sqrt{\phi^2 - \lambda^2}} \quad (29)$$

where  $\chi$  is the reduction factor;  $\lambda$  is the non-dimensional slenderness;

$$\phi = 0.5[1 + \alpha(\lambda - 0.2) + \lambda^2] \quad (30)$$

$\alpha$  is the imperfection factor for buckling curve given in *Eurocode 3* ( $\alpha=0.21$ ) [10\*]. Then on dimensional slenderness  $\lambda$  for the bending plane is expressed as :

$$\lambda = \sqrt{N_u/N_{cr}} \leq 2 \quad (31)$$

$$N_u = f_y A_s + f_{yr} A_{sr} + \nu A_c f_c' \quad (32)$$

$$N_{cr} = \pi^2 (EI)_{eff} / Le^2 \quad (33)$$

$$(EI)_{eff} = E_s I_s + E_{sr} I_{sr} + 0.6 E_{cm} I_c \quad (34)$$

Where  $N_u$  is the nominal section capacity,  $\nu=1$  for a CFST and  $\nu=0.85$  for encased column,  $N_{cr}$  = the elastic critical normal force,  $(EI)_{eff}$  = The effective flexural stiffness,  $E_s$  = the elastic modulus of steel;  $E_{cm}$  = the secant modulus of elasticity for concrete.

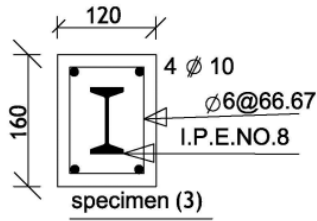
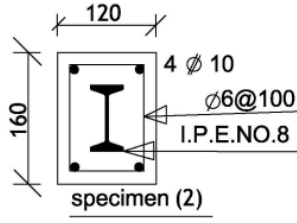
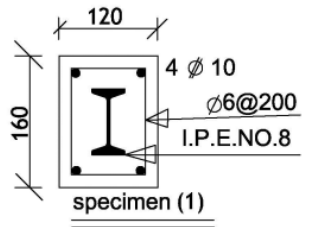
## II. EXPERIMENTAL PROGRAM

### 2.1. Characteristics of test specimens

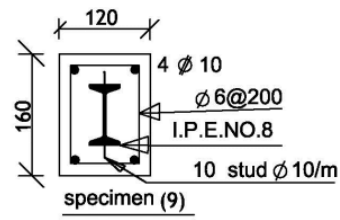
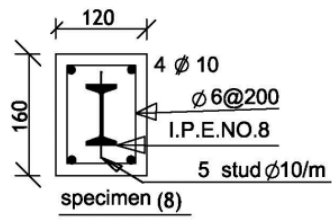
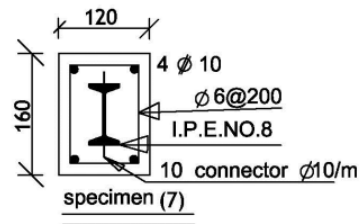
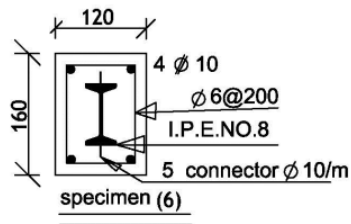
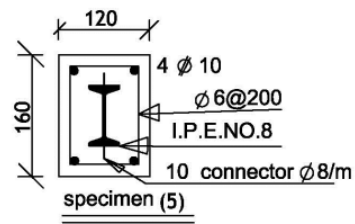
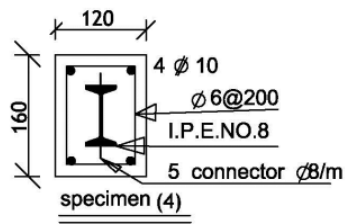
Nine specimens encased steel composite concrete columns were designed to investigate the effect of the tested parameters which are the concrete contribution, the concrete confinement using different stirrups ratio and shear connector as well as different types of connectors diameter or spacing between connectors. Determination of the axial capacity portion for both steel and concrete section is also investigated. The concrete compressive strength,  $f_{cu}$  was 53.7 MPa for all columns. All columns had rectangular cross section of size 120\*160mm and were longitudinally reinforced by 4 bars of 10 mm diameter. With entire height 1100mm. The tested columns are divided into two main groups according to spacing between stirrups and the shear connectors types, diameters and numbers. Column  $C_1$  is considered as control specimens. The details of the tested specimens are illustrated in table 1 and fig. 1, 2.

**Table 1: Shows the properties of tested composite column,  $f_{cu}=53.7\text{Mpa}$**

Spec. No.	Diment. (mm)	Main. RFT.	Stir.	Steel sect.	Shear Connectors	Ac (net) mm <sup>2</sup>	Asr mm <sup>2</sup>	Ass mm <sup>2</sup>
1	120×160	4Ø10	5 φ6/m	Steel I.P.E No.8	-----	18436	314.16	764
2	120×160	4Ø10	10 φ6/m	Steel I.P.E No.8	-----	18436	314.16	764
3	120×160	4Ø10	15 φ6/m	Steel I.P.E No.8	-----	18436	314.16	764
4	120×160	4Ø10	5 φ6/m	Steel I.P.E No.8	connector 5 φ 8/m	18436	314.16	764
5	120×160	4Ø10	5 φ6/m	Steel I.P.E No.8	connector 10 φ 8/m	18436	314.16	764
6	120×160	4Ø10	5 φ6/m	Steel I.P.E No.8	connector 5 Φ 10/m	18436	314.16	764
7	120×160	4Ø10	5 φ6/m	Steel I.P.E No.8	connector 10 Φ 10/m	18436	314.16	764
8	120×160	4Ø10	5 φ6/m	Steel I.P.E No.8	5 stud φ 10/m	18436	314.16	764
9	120×160	4Ø10	5 φ6/m	Steel I.P.E No.8	10 stud φ 10/m	18436	314.16	764



**specimens show the effect of confinement**



**specimens show the effect of shear connectors**

Fig. 1: Details of the tested columns

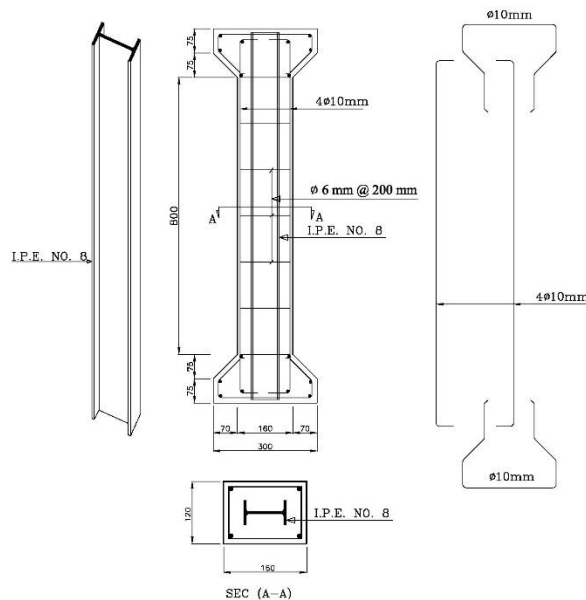


**Fig. 2: Column specimen dimension and reinforcement**



**Fig. 3: Details of confining columns and shear connectors**

## 2.2. Material Properties

The used concrete mix for casting all the columns was produced from ordinary Portland cement, natural sand and crushed dolomite with a maximum nominal size of 10 mm. The columns were demolded after 24 h from casting, covered with wet burlap and stored under the laboratory conditions for 28 days before proceeding to testing stage. Clean drinking fresh water was used for mixing and curing the specimens. High grade steel (36/52) of diameter 10 mm and normal mild steel bars St 24/37-smooth bars of diameter 6 mm were used for longitudinal reinforcement and stirrups respectively. The yielding strength,  $f_y$  of encased sections was 240 MPa (St24/37). The concrete mix used in all specimens was designed according to the Egyptian code of practice. The concrete mix was designed to obtain target strength of 53.7 N/mm<sup>2</sup> at the age of 28 days.

## 2.3. Confinement and Shear Connectors Techniques

### 2.3.1. CONFINEMENT:

Increasing in number of horizontal stirrups technique is used in the present study to investigate the effect of confinement on column load carrying capacity.

Three different specimens are used to clear the increasing numbers of stirrups technique:

- Column C<sub>1</sub> is considered as the controlled specimen. The numbers of stirrups (that is used in it) are 5Ø 6 mm / m.
- Column C<sub>2</sub> contains horizontal stirrups of 10 Ø 6 mm / m.
- Column C<sub>3</sub> contains horizontal stirrups of 15 Ø 6 mm / m.

### 2.3.2. SHEAR CONNECTORS:

In the present study it was used the technique of different types, numbers and diameters of horizontal shear connectors welded to steel section to investigate the effect of shear connectors on column load carrying capacity with the constant of stirrups numbers.

Three different groups of specimens are used in shear connector's technique:

- Columns C<sub>4</sub>, C<sub>5</sub> contain connectors of normal mild steel bars with grade 24/37-smooth bars of diameter 8 mm with different numbers of 5 Ø 8 mm / m and 10 Ø 8 mm / m for C<sub>4</sub>, C<sub>5</sub> respectively.
- Columns C<sub>6</sub>, C<sub>7</sub> contain connectors of high grade steel 36/52 of diameter 10 mm with different numbers of 5 Φ 10 mm / m and 10 Φ 10 mm / m for C<sub>6</sub>, C<sub>7</sub> respectively.

- Columns C<sub>8</sub>, C<sub>9</sub> contain Stud's shear connectors of normal mild steel with grade 24/37-smooth bars of diameter 10 mm with different numbers of 5 Ø 10 mm /m and 10 Ø 10 mm /m for C<sub>8</sub>, C<sub>9</sub> respectively, as shown in fig. 1, fig. 3 and table 1.

#### 2.4. STRAIN GAUGES and LVDTs

Five strain gauges have been used inside of mid height for all specimens, two were mounted on two vertical steel bars (BAR I) and (BAR II), another one was mounted on the stirrup (BAR III), one was mounted on the web of steel section (BAR IV). And one was mounted on the flange of steel section (BAR V). Two linear variable differential transducers (LVDT) have been used to measure the columns deformations during loading. The gauge length was chosen at vertical direction (LVDT1) equal to 640 mm to represent the axial deformation of the column and at horizontal direction (LVDT2) equal to 130mm to represent the lateral deformation of the column.

Fig. 4 shows the location of internal strain gauges and external LVDTs.

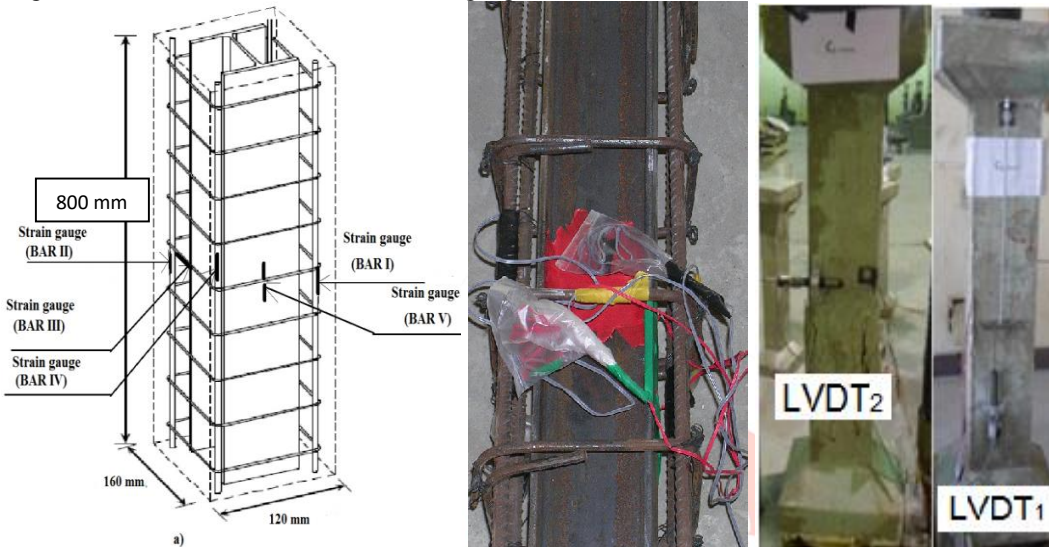


Fig. 4: Location of strain gauges and LVDTs.

#### 2.5. Test Setup and Procedure

All column specimens were tested under static compression axial loads using the testing machine mounted on the material laboratory of Al-Azhar University, which has an ultimate compressive load capacity of 2000kN. The data were collected automatically by using a data acquisition system as shown in fig. 5 which represents the schematic diagram of the test setup. Prior to the test, each column was centered at the machine head and an initial load was applied to ensure concentric loading. All the columns were tested up to failure which was recognized when a sudden drop in the applied load was reached. This pattern of gages allows for accurate axial strain measurements and traces any unintended eccentricity.

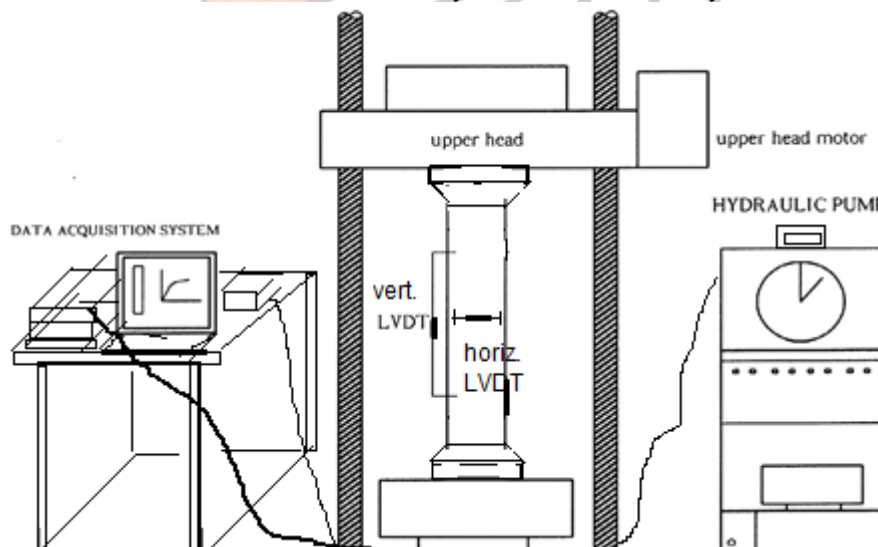


Fig. 5 Schematic diagram of the test setup for the tested columns.

### III. EXPERIMENTAL TEST RESULTS

Table 2 show experimental results of the tested columns that the ultimate load  $P_u$ , the corresponding deformation, the ductility factor  $\mu$ , Poisson's ratio  $\psi$ , toughness, stiffness and the column load carrying capacity as a percentage of control columns. Table 3 show the strain and forces in internal reinforcement and steel section.

**Table 2: Experimental results of the tested columns.**

Col No.	$P_u$ (kN)	Column Carrying Capacity (% of control)	$\Delta_u$ (mm)	$\Delta_f^a$ (mm)	$\Delta_y^b$ (mm)	$\mu^c$	$\psi^d$	Modulus of toughness (N/mm <sup>2</sup> )	Stiffness (N/mm <sup>2</sup> )
C1	975.5	100%	2.410	2.900	1.894	1.203	0.700	0.200	12872.98
C2	1003.38	103%	2.502	3.890	1.290	1.554	0.520	0.278	19182.83
C3	1118.3	115%	2.600	4.975	0.795	1.913	0.152	0.396	37672.43
C4	976.86	100.14%	1.500	1.755	0.920	1.170	0.144	0.122	22930.98
C5	980.66	100.53%	1.696	1.994	1.031	1.176	0.309	0.139	23886.68
C6	1056.42	108.3%	1.400	1.901	0.375	1.358	0.799	0.143	26409.21
C7	1056.42	108.3%	1.491	2.412	0.806	1.618	4.486	0.181	29345.29
C8	1046	107.23%	3.005	3.686	1.294	1.227	0.770	0.274	20408.55
C9	1047.58	107.4%	3.050	3.780	1.320	1.239	0.780	0.282	21494.90

<sup>a</sup>  $\Delta_f$  is the deformation corresponding to a load equal to 75% of the ultimate load on the descending branch of the load-deformation curve.

<sup>b</sup>  $\Delta_y$  is the deformation corresponding to the intersection of the secant stiffness at a load equal to 75% of the ultimate load and the tangent at the ultimate load.

<sup>c</sup>  $\mu$  is the ductility factor =  $(\Delta_f / \Delta_u)$ .

<sup>d</sup>  $\psi$  is the Poisson's ratio = Lateral Strain ( $\epsilon_{laterally}$ ) / Longitudinal Strain ( $\epsilon_{longitudinally}$ )

**Modulus of toughness (N/mm<sup>2</sup>) = total area under stress strain curve till strain corresponding to a stress equal to 75% of the ultimate stress on the descending branch of the stress-strain curve.**

**Stiffness (N/mm<sup>2</sup>) is the slope of stress- strain curve in the elastic zone**

It can be seen that increasing numbers of steel stirrups used in confining columns (C2, C3) gives an increase in the column load carrying capacity, ductility, stiffness and modulus of toughness but decrease the Poisson's ratio of columns. However, the ultimate load of columns with high strength bars ( $\Phi 10$ ) shear connectors welded to flange steel sections (C6, C7) were higher than that of columns with other types of shear connectors. Also, the ultimate load of columns with mild steel stud ( $\phi 10$ ) welded to flange steel sections (C8, C9) were higher than that of columns with smooth bars (mild steel ( $\phi 8$ )) welded to flange of steel sections. It is also noted that increasing the number of shear connectors that used in columns with shear connectors from 5/m to 10/m led to increase in the ductility factor, Poisson's ratio, modulus of toughness and stiffness for all types of shear connectors, as shown in table 2.

**Table 3: Experimental strain and forces in internal reinforcement and steel section.**

Col. No.	Strain value ( $\times 10^{-6}$ ) in vertical R.F.T (BAR I), (BAR II)	Equiv. force in one vertical R.F.T (KN)	Strain value ( $\times 10^{-6}$ ) in stirrups (BAR III)	Equiv. force in stirrups (KN)	Strain value ( $\times 10^{-6}$ ) in web (BAR IV)	Equiv. force in web (KN)	Strain value ( $\times 10^{-6}$ ) in flange (BAR V)	Equiv. force in one flange (KN)	Equiv. force in concrete (KN)
C1	-2932.26	-48.59	440.82	2.63	-1577.50	-88.03	-1674.84	-88.26	516.57
C2	-2748.35	-45.55	830.46	4.95	-1580.57	-88.20	-1324.15	-69.78	593.43
C3	-2714.64	-44.99	1045.03	6.23	-1515.82	-84.59	-1292.08	-68.09	717.58
C4	-1804.89	-29.91	641.54	3.83	-1093.89	-61.04	-970.91	-51.17	693.84
C5	-1340.98	-22.22	1049.62	6.26	-1360.84	-75.94	-1350.78	-71.19	673.46
C6	-1873.56	-31.05	1111.82	6.63	-1530.52	-85.41	-1453.07	-76.58	693.66
C7	-2078.54	-34.45	1186.43	7.08	-1460.26	-81.49	-1978.02	-104.24	628.67
C8	-2247.04	-37.24	199.45	1.19	-2149.17	-119.93	-2149.17	-113.26	550.59
C9	-1553.50	-25.74	424.20	2.53	-1545.31	-86.24	-1603.55	-84.51	689.35



Table 3 shows the experimental strains and equivalent forces in all elements of tested columns (vertical reinforcement, horizontal stirrups, steel section and concrete).

### 3.1. Crack pattern and mode of failure

During testing, the columns surfaces were observed in order to follow the development and the propagation of cracks. The appearance of these cracks was always a sign that the column has attained the failure state. The failure mechanisms of the tested columns without shear connector at the encased steel section were almost the same. The damage sequence for columns was as follows: inclined cracks occurred at the upper or lower part of the column and with increasing of the applied load cracks became wider and the cover started to spall off. Finally, crushing of concrete occurred followed by buckling of vertical steel reinforcement. As in the samples with shear connector at the encased steel sections were happening distribution of cracks in most high column, was clearly seen in the sample C7, Fig. 6 shows the crack patterns and the mode of failure of the tested columns.

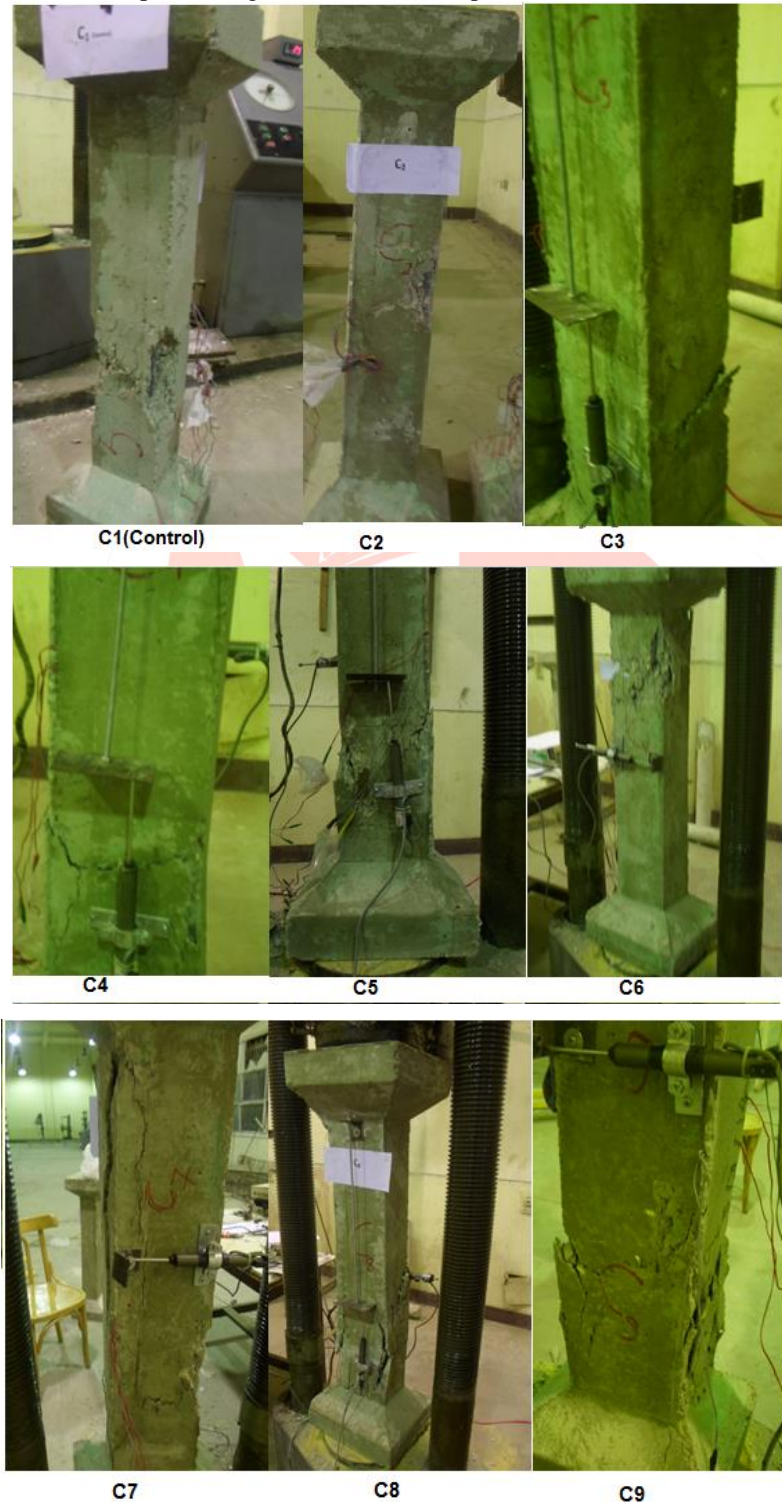
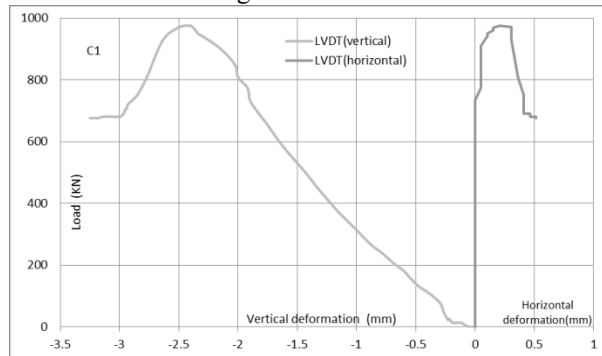


Fig. 6: Failure patterns of the tested columns.

**3.2. Load- deformation relationship:**

Fig. 7 to 15 shows the axial load versus average concrete vertical and horizontal deformation for all the tested columns. The curves start with a linear part. At stress levels near the ultimate stress of concrete, the curves start to bend indicating that the concrete had cracked and the stirrups started their confining action.



**Fig. 7: Load versus deformation for column (C1)**

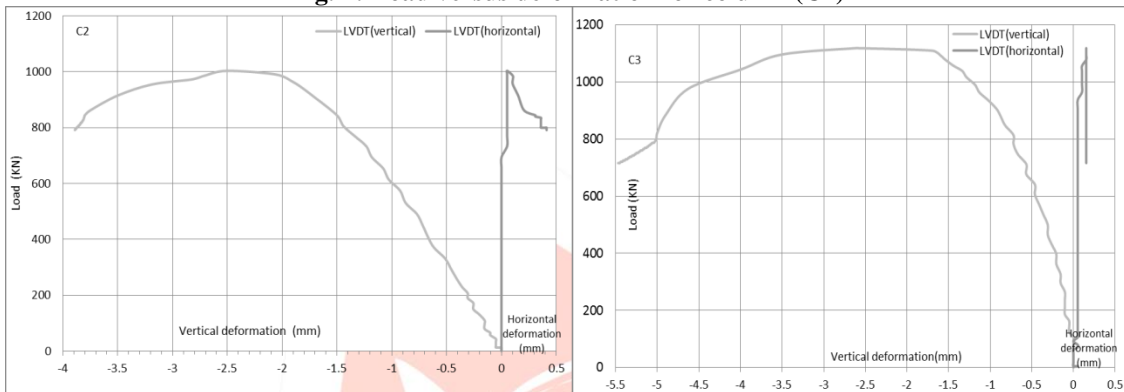


**Fig. 8: Load versus deformation for column (C2)**

**Fig. 9: Load versus deformation for column (C3)**

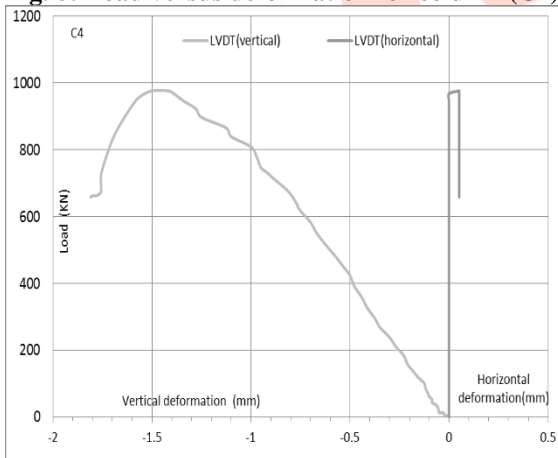


**Fig.10: Load versus deformation for column (C4)**

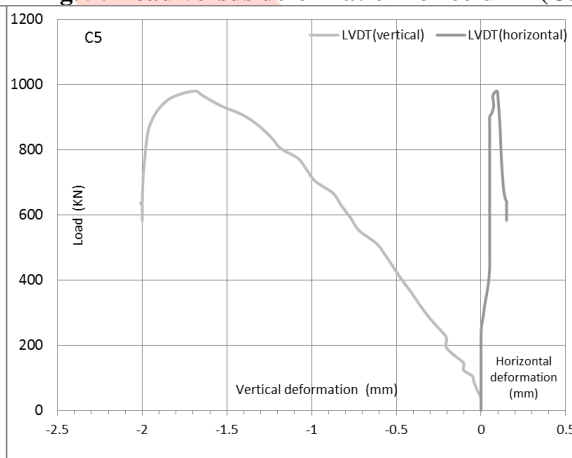


**Fig. 11: Load versus deformation for column (C5)**

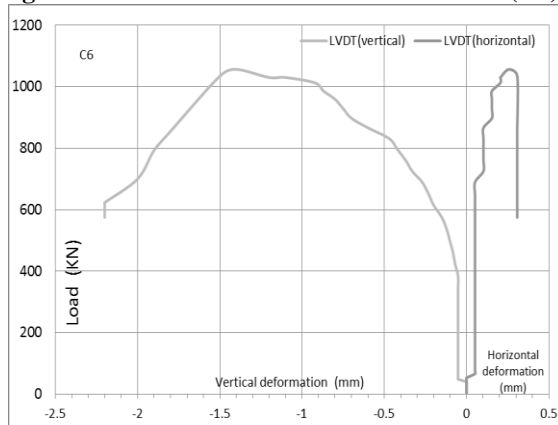


**Fig. 12: Load versus deformation for column (C6)**

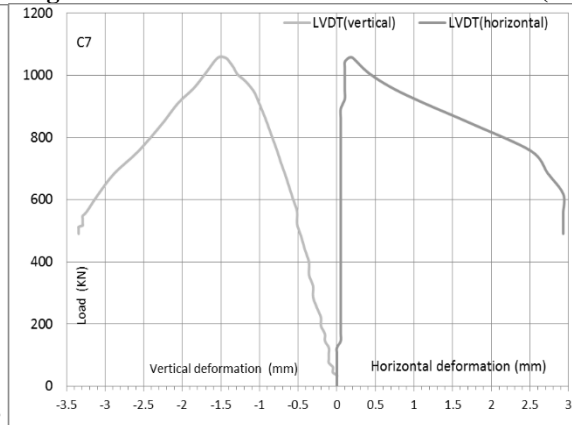


**Fig. 13: Load versus deformation for column (C7)**

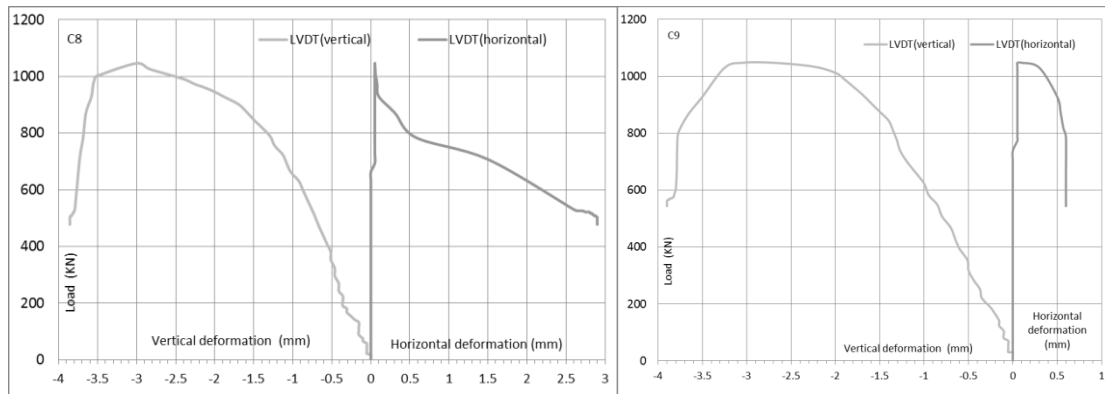


**Fig. 14: Load versus deformation for column (C8)** **Fig. 15: Load versus deformation for column (C9)**

**3.3. Strains in steel reinforcement:**

The strains in vertical reinforcement of the tested specimens reached yielding at the ultimate load. However the observations at failure showed that the yielding of stirrups might have occurred. The measured steel strain is shown in fig. 16 a, b, c.

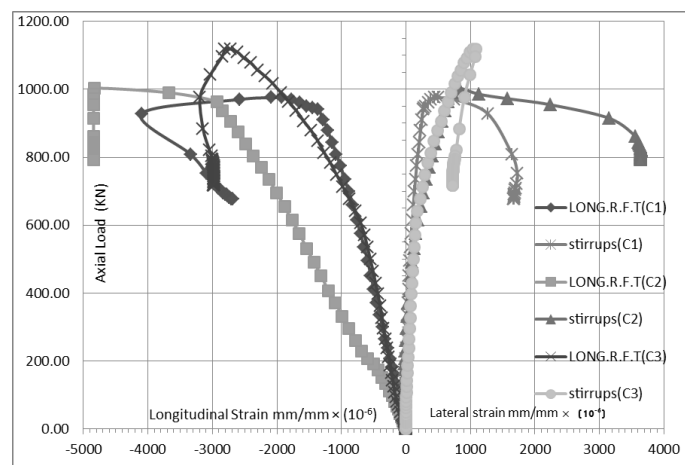


**Fig. 16. a: Load versus steel strain for tested columns (C1:C3)**

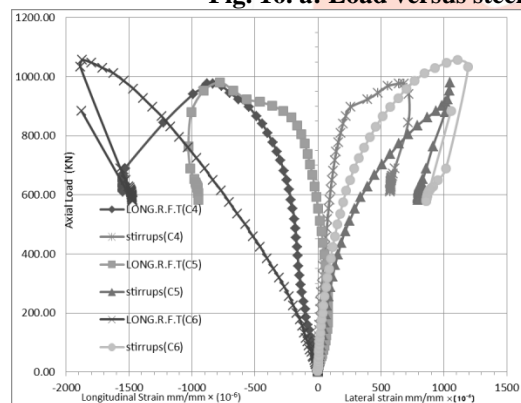


**Fig. 16. b: Load versus steel strain for tested columns (C4:C6)**

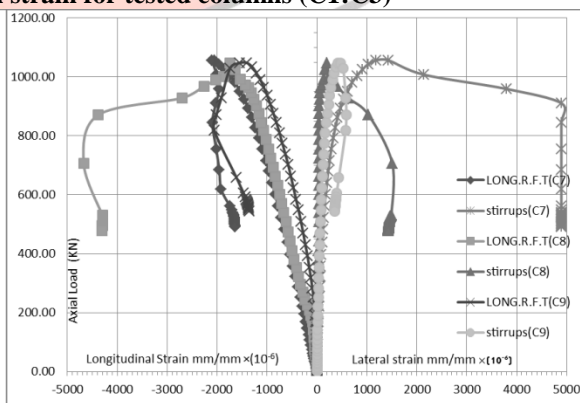


**Fig. 16. c: Load versus steel strain for tested columns (C7:C9)**

Based on all the previous measurements, it is obvious that the ultimate load, corresponding deformation and strains of steel for the tested columns varied depending on both the configuration of the lateral steel reinforcement and the shear connectors welded in encased steel shapes which are not considered in the available design codes.

**IV. THEORETICAL EVALUATION OF THE EXPERIMENTAL RESULTS**

This paper investigates and evaluates the ultimate axial compression strength of the concrete encased steel columns and also the concrete contribution to the ultimate axial load according to the available different codes. For each specimen, the loads carried by the concrete portion, steel portion, and the composite section were determined according to the available different codes [1–8] requirements. All the partial factors of safety for materials and the resistance factors are set to unity. This will give an unbiased comparison of the capacities predicted by the eight methods since each method has its own resistance factors which are used with the corresponding load factors. The calculated capacities are presented in table 4 and compared to the experimental results as shown in Table 5. The main equations used in the analysis are mentioned above for each code:

**Table 4: Calculated axial capacities of the tested columns according to available codes  $P_{calc.}$ ,  $P_u$  (EXP.), kN.**

Col. No.	$P_u$ (EXP.)	ECP203-2007 [1]	ECPSCLRFD - 2012 [2]	ACI-318 [3]	AISC-LRFD-2010 [4]	BS540 0-5 [5]	Chinese code CECS159 [6]	Hong Kong code [7]	Euro code4 [8]
C1	975.50	545.131	562.142	824.22	604.1	710.76	781.91	685.12	709.58
C2	1003.38								
C3	1118.30								
C4	976.86								
C5	980.66								
C6	1056.42								
C7	1056.42								
C8	1046.00								
C9	1047.58								

**Table 5: Comparison between calculated axial capacities of the tested columns and experimental results, ( $P_u$  (EXP.)/ $P_{calc.}$ )**

Column No.	ECP203-2007 [1]	ECPSCLRFD - 2012 [2]	ACI-318 [3]	AISC-LRFD-2010 [4]	BS5400-5 [5]	Chinese code CECS159 [6]	Hong Kong code [7]	Eurocode4 [8]
C1	1.789	1.735	1.184	1.615	1.372	1.248	1.424	1.375
C2	1.841	1.785	1.217	1.661	1.412	1.283	1.465	1.414
C3	2.051	1.989	1.357	1.851	1.573	1.430	1.632	1.576
C4	1.792	1.738	1.185	1.617	1.374	1.249	1.426	1.377
C5	1.799	1.745	1.190	1.623	1.380	1.254	1.431	1.382
C6	1.938	1.879	1.282	1.749	1.486	1.351	1.542	1.489
C7	1.938	1.879	1.282	1.749	1.486	1.351	1.542	1.489
C8	1.919	1.861	1.269	1.732	1.472	1.338	1.527	1.474
C9	1.922	1.864	1.271	1.734	1.474	1.340	1.529	1.476
Aver.	1.888	1.831	1.248	1.703	1.448	1.316	1.502	1.450

**Table 6: Concrete contribution ratio due to the experimental results and available codes.**

Column No.	Exp. data	ECP 203-2007 [1]	ECPSCLRFD -2012 [2]	ACI-318 [3]	AISC-LRFD-2010 [4]	BS540 0-5 [5]	Chinese code CECS159 [6]	Hong Kong code [7]	Eurocode4 [8]
C1	0.53	0.67	0.65	0.69	0.69	0.63	0.68	0.63	0.614
C2	0.59	0.67	0.65	0.69	0.69	0.63	0.68	0.63	0.614
C3	0.64	0.67	0.65	0.69	0.69	0.63	0.68	0.63	0.614
C4	0.71	0.67	0.65	0.69	0.69	0.63	0.68	0.63	0.614
C5	0.69	0.67	0.65	0.69	0.69	0.63	0.68	0.63	0.614
C6	0.66	0.67	0.65	0.69	0.69	0.63	0.68	0.63	0.614
C7	0.60	0.67	0.65	0.69	0.69	0.63	0.68	0.63	0.614
C8	0.53	0.67	0.65	0.69	0.69	0.63	0.68	0.63	0.614
C9	0.66	0.67	0.65	0.69	0.69	0.63	0.68	0.63	0.614

Referring to table 4, it is noticed that the calculated axial capacities of the first three specimens are the same as the used codes do not considering the confinement effect for predicting the ultimate axial strength. So, to predict the effect of confinement one from the following formulas can be used:

-The formula of *Egyptian Code for FRP* [17] that presents the following equation for the strength of confined columns:

$$f_{cuc} = f_{cu} \left[ 2.25 \sqrt{1 + 9.875 \frac{f_l}{f_{cu}}} - 2.25 \frac{f_l}{f_{cu}} - 1.25 \right] \quad (35)$$

Where:  $f_{cuc}$  = the compressive strength of confined concrete.  $f_{cu}$  = the specified compressive strength of concrete.

-The formula of *Mander et al.* [18] that presents the following equation for the strength of confined columns:

$$f'_{cc} = f'_{co} \left( -1.254 + 2.254 \sqrt{1 + \frac{7.94 f'_l}{f'_{co}}} - 2 \frac{f'_l}{f'_{co}} \right) \quad (36)$$

Where:  $f'_{cc}$  = the compressive strength of confined concrete =,  $f'_{co}$  = the compressive strength of unconfined concrete =  $f'_c$ ,  $f'_l$  = the effective lateral confining stress =  $f_l = f_r$ .

-The formulas of *O'Shea and Bridge [19]* that:

$$f_{cc} = f_c' [-1.228 + 2.172 \sqrt{1 + \frac{7.46 f_r}{f_c'}} - 2 \frac{f_r}{f_c'}] \text{ for } f_c' \leq 50 \text{ MPa} \tag{37}$$

$$f_{cc} = f_c' \left[ \frac{f_r}{0.558 \sqrt{f_c'}} + 1 \right]^{1.25(1+0.062 \frac{f_r}{f_c'})} (f_c')^{-0.21} \text{ for } 80 < f_c' < 100 \text{ MPa} \tag{38}$$

Where  $f_l$  is calculated according to the shape and strengthening system of cross-section we can calculate it as shown in fig. 17

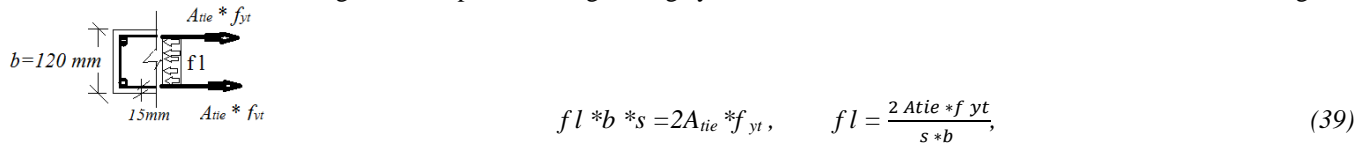


**Fig. 17: lateral pressure due to stirrups.** Where: s = spacing between stirrups (*ties*).

**Table 7 Compressive strength of confined concrete by stirrups and Pu (KN), ECP203-2007 [1]**

Column No.	S (mm)	Confined compressive strength of concrete (Mpa) [17]	Pu (KN), ECP203-2007 [1]	Ultimate column. carrying capacity(%) of control	Confined compressive strength of concrete (Mpa) [18]	Pu (KN), ECP203-2007 [1]	Ultimate column. carrying capacity(%) of control
C1	200	59.92	585.264	100%	58.76	577.78	100%
C2	100	65.659	622.297	106.3%	63.5	608.37	105.3%
C3	66.67	70.995	656.728	112.2%	67.96	637.145	110.3%
C4: C9	200	59.92	585.264	100%	58.76	577.78	100%

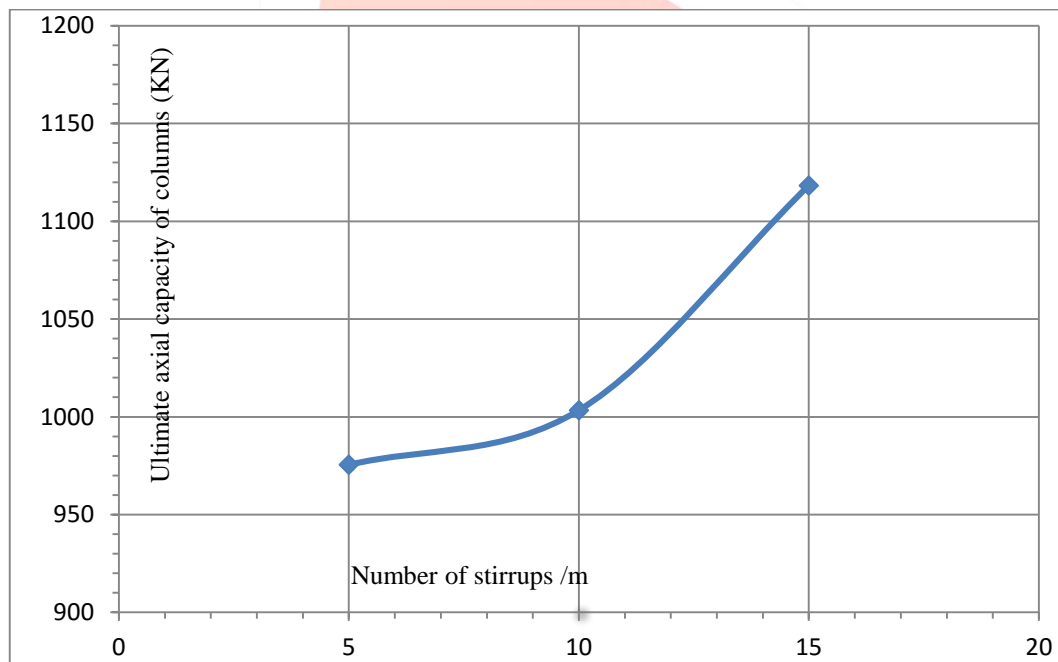


**Fig. 18: Experimental ultimate axial capacity versus number of stirrups for tested columns**

**Table 8: Load transfer due to the experimental results and available codes, KN**

Column No.	Exp. Data	AISC-LRFD-2010 [4]
C1	264.56	296.089
C2	227.77	304.552
C3	220.77	339.433
C4	163.38	296.502
C5	218.31	297.655
C6	238.56	320.65
C7	289.97	320.65
C8	346.45	317.488
C9	255.25	317.967

Referring to Table 5, the comparative studies with the experimental results show that the predicted results are generally lower than the test results which mean that the calculated column strengths using the previous codes are almost on the conservative side. ACI-318 [3] gives the closest prediction with an average of 24.8% lower than the test results and ECP203-2007 [1] gives the most conservative results with an average of 88.8% lower than the test results. On the other hand, the calculated ratios of concrete contribution ranged between 0.63 and 0.70 according to codes [1- 8], and it varied from 0.53 to 0.71 according to experimental results, see Table 6. It is clear that considerable discrepancies exist between codes and the experimental data due to neglecting of the stirrups confinement and the effect of shear connectors that welded to encased steel shape in these codes, where the calculated concrete contribution of the specimens are the same as the used codes do not considering the effect of confinement and shear connector. Also, it is noticed that the enhancement of the experimental concrete contribution of columns due to the confinement effect and presence of shear connectors.

Table 7 shows enhancement of the theoretical ultimate axial capacity of columns with taking into consideration the effect of the confinement. Also, it can be seen that increasing the stirrups from 5  $\emptyset$  6 mm / m to 10  $\emptyset$  6 mm / m and from 10  $\emptyset$  6 mm / m to 15  $\emptyset$  6mm / m increase the ultimate column carrying capacity by (5 – 6) % approximately.

Table 8 shows the values of a compression between the theoretical and experimental shear transfer between concrete and steel shapes. This force transfer by shear connectors in the columns with shear connectors. Referring to fig. 18, the experimental ultimate axial capacity versus number of stirrups for tested confined columns. It can be seen that the ultimate load of C2 was 2.86% higher than that of C1 and the ultimate load of C3 was 11.45% higher than that of C2.

## V. CONCLUSIONS

From the present study, the followings have been concluded:

1. A non-negligible difference between the available codes of practice and the experimental results is shown. The introduction of confinement coefficients and shear connectors has an influence on the ultimate calculated axial loads.
2. The calculated column strengths using the available previous codes are found to be mostly conservative when compared with the experimentally obtained test results. ACI-318 [3] gives the closest prediction with an average of 24.8% lower than the test results and ECP203-2007 [1] gives the most conservative results with an average of 88.8% lower than the test results.
3. The values of confinement coefficients need to be adjusted in the used codes as they neglect the increase in strength, ductility and stiffness of columns due to transverse ties.
4. The obtained results show that the Increasing numbers of steel stirrups used in confining columns gives an increase in the load carrying capacity of columns. Where, it was noted that when the number of stirrups increased from 5  $\emptyset$  6 mm/m to 15  $\emptyset$  6 mm/m the maximum experimental load of column increased about (15%).
5. The adding of shear connectors inside the columns welding in the flange of steel sections increased the column carrying capacity, where the largest increasing in bearing capacity of tested columns a ratio of control column was for columns that use connectors in the form of high strength bars and diameter of ( $\Phi$ 10 mm) with an increase of 8.3 %.
6. Using stud's shear connectors with diameter of (10 mm) increase the capacity by 7.4%, but the columns with connectors in the form of smooth bars and diameter of ( $\emptyset$ 8 mm) were small increase of 0.53 %, therefore, it is preferred to use the connectors in the form of high strength bars types from other types in the present study.
7. The concrete contribution is mainly dependent on the number of ties and shear transfer between the concrete and steel sections. Despite this, no specific requirements for calculating shear transfer between the encased steel section and concrete are available in the design codes. Future researches need to cover this point.
8. Finally, under axially loading, the deformation and mechanical performance of the concrete encased steel column with shear connectors can further study with different factors, such as length to width ratio, slenderness ratio, axially load level and age, strength of concrete, strength and shape of encased steel section, and also can analyze the influences of ultimate bearing capacity under different factors by the orthogonal experiment.

## VI. ACKNOWLEDGEMENT

The researchers express their gratitude to the staff of “faculty of engineering, Al-Azhar University and Reinforced Concrete Institute Housing and Building National Research Centre”, for their great effort through all experimental stages of this research.

## REFERENCES

- [1] Egyptian Code of Practice for Design and Construction of Concrete Structures, ECP 203, Housing and Building National Research Center, 2007.
- [2] Egyptian Code of Practice for Steel Construction (ECP-SC-LRFD-2012).
- [3] Building Code Requirements for Reinforced Concrete, American Concrete Institute, ACI 318, Detroit, 2008.
- [4] Specification for Structural Steel Buildings, (AISC-LRFD), American Institute of Steel Construction, Chicago, Illinois, 2010.
- [5] Steel, Concrete and Composite Bridges, Part 5, (BS.5400-5): Code of Practice for Design of Composite Bridges, 2002.
- [6] CECS159. Technical specification for structures with concrete filled rectangular steel tube members. Beijing: China Planning Press; 2004 (in Chinese).
- [7] Code of Practice for the Structural Use of Steel 2011. Hong Kong: Buildings Department; 2011.
- [8] Eurocode4. Design of composite steel and concrete structures, part 1.1: general rules and rules for buildings. London: British Standards Institution; 2004.
- [9]- S. El - Tawil, G. Gregory. Strength and ductility of concrete encased composite columns. J. Struct. Eng 1999; 125: 1009–1019.

- [10]- C. Weng, S. Yen. Comparisons of concrete - encased composite column strength provisions of ACI code and AISC specification. *Eng. Struct.* 2002; 24:59 – 72.
- [11]-N. Shanmugam, B. Lakshmi. State of the art report on steel–concrete composite columns. *J. Constr. Steel Res.* 2001; 57: 1041–1080.
- [12] K.Z. Soliman, A.I. Arafa, Tamer M. Elrakib. Review of design codes of concrete encased steel short columns under axial compression. *HBRC Journal* 2013; 9: 134–143, Cairo, Egypt.
- [13]- M. Mimoune. Design of Steel Concrete Composite Columns Subject to Axial Compression. *Constantine University Algeria* 2010; 35: 201–207.
- [14]- A. Paul, A. Samanta .Review of design practice of concrete encased steel short column under axial load. *Int. J. Earth Sci. Eng.* 2011; 4: 608–611.
- [15]- Amiya Kumar Samanta , Amit Paul . Evaluation of Current Design Practices on Estimation of Axial Capacity of Concrete Encased Steel Composite Stub Columns: A Review. *Journal of Civil Engineering and Architecture* 2013; 7: 1080-1091, USA.
- [16] Laith Khalid Al- Hadithy, Khalil Ibrahim Aziz, Mohammed Raji M. AL-Alusi. Experimental And Finite Element Investigation On The Load–Slip Behavior Of Composite Push Out Segments Using Various Shear Connectors. *Journal of Engineering* 2009; 15: 4087- 4111.
- [17]- Egyptian Code for FRP; (Code 208Version 2005), Chapter 2 and Chapter3.
- [18] Mander. J. B, Priestley, M. J. N, Park, R. Theoretical Stress- Strain Model for Confined Concrete. *Journal of Structural Engineering, ASCE*1988; 114: 1804-1826.
- [19]- O’Shea, M. D., and Bridge, R. Q. Design of circular thin-walled concrete filled steel tubes, *Journal of Structural Engineering* 2000; 126: 1295-1303.

